

Received: 2017.11.07
Accepted: 2018.01.08
Published: 2018.02.12

Angiotensin-Like 4 Attenuates Brain Edema and Neurological Deficits in a Mouse Model of Experimental Intracerebral Hemorrhage

Authors' Contribution:
Study Design A
Data Collection B
Statistical Analysis C
Data Interpretation D
Manuscript Preparation E
Literature Search F
Funds Collection G

ABCDEF 1 **Zhandong Qiu**
BCDE 2 **Jia Yang**
BCD 1 **Gang Deng**
EF 3 **Yu Fang**
EF 3 **Dayong Li**
AG 1,4 **Suming Zhang**

1 Department of Neurology, Tongji Hospital of Tongji Medical College, Huazhong University of Science and Technology, Wuhan, Hubei, P.R. China
2 Department of Neurology, Beijing Friendship Hospital, Capital Medical University, Beijing, P.R. China
3 Department of Emergency Medicine, Tongji Hospital of Tongji Medical College, Huazhong University of Science and Technology, Wuhan, Hubei, P.R. China
4 Shenzhen Research Institute of Huazhong University of Science and Technology, Shenzhen, Guangdong, P.R. China

Corresponding Author: Suming Zhang, e-mail: sumingzhang123@163.com

Source of support: This work was supported by the Fund of Shenzhen Science & Technology Plan Projects (No. JCYJ20140509162710497) and the Fund of National Natural Science Foundation of China (NSFC 81271407)

Background: Angiotensin-like 4 (ANGPTL4) is neuroprotective when administered acutely for the treatment of cerebral ischemia. The aim of the present study was to evaluate the preventive effects of ANGPTL4 on the formation of brain edema and to determine whether it promotes the recovery of neurological function following intracerebral hemorrhage (ICH).





Material/Methods: Recombinant human ANGPTL4 (rhANGPTL4; 40 µg/kg) or a vehicle was administered intraperitoneally 5 min prior to bacterial collagenase-induced ICH in male C57/B6J mice. Behavioral tests were performed prior to ICH and at days 1, 3, 7, 14, 21, and 28 after ICH. Brain edema and hematoma volume were examined separately using the wet weight/dry weight method and hematoxylin-eosin staining. The integrity of the tight and adherens junctions was quantified via immunofluorescence. The ultrastructure of the blood-brain barrier (BBB) was examined using transmission electron microscopy. Vascular endothelial (VE)-cadherin, claudin-5, Src, and phospho-Src in the ipsilateral and contralateral striatum were detected by Western blot analysis.

Results: RhANGPTL4 reduced brain edema and hematoma volume and improved neurological functional recovery over the subsequent 4 weeks when compared with the control group. rhANGPTL4 significantly increased VE-cadherin and claudin-5-positive areas and relative amounts in the peri-hematoma region compared with the control group. In addition, ANGPTL4 significantly reduced the ratio of phospho-Src to Src. The significant reduction of Src kinase activity in the peri-hematoma region of ANGPTL-treated mice was paralleled by a decrease in vascular permeability and edema formation.

Conclusions: These results suggest that ANGPTL4 is a relevant target for vasculoprotection and cerebral protection during stroke.

MeSH Keywords: **Blood-Brain Barrier • Brain Edema • Cerebral Hemorrhage**

Full-text PDF: <https://www.medscimonit.com/abstract/index/idArt/907939>

 3785  —  5  37



Background

Intracerebral hemorrhage (ICH) accounts for 20–30% of strokes in Asia [1] and is associated with high mortality rates [2]. ICH has an annual incidence of 10–30 cases per 100 000 people, which is increasing and is expected to double by the year 2050 [3]. Therefore, novel techniques and treatments are required to ameliorate the risks of profound morbidity and mortality associated with spontaneous intracerebral hemorrhage; however, thus far, no effective treatments have been developed.

Although the mechanism of injury and therapeutic targets of ICH have previously been investigated, many clinical trials based on preclinical data have been unsuccessful [4]. Various forms of edema occur because of ICH, with vasogenic edema being the principal form [5]. Perihematoma edema has also been implicated as a contributing factor to delayed neurological deterioration after ICH [6]. One study indicated that the time course of the neurological deficit closely matched the time course of cerebral edema for ICH in a rat model [7]. Following ICH or ischemia/reperfusion, the blood-brain barrier (BBB) becomes more permeable, promoting increased infiltration of proinflammatory cells and the blood components thrombin and lysed red blood cells, which ultimately results in perihematomal edema formation [5,8].

Over the last decade, it has been determined that angiotensin-like protein 4 (ANGPTL4) plays a role in lipid metabolism, tumorigenesis, angiogenesis, and redox regulation [9]. A previous study demonstrated that ANGPTL4 treatment provides a vasculoprotective effect, counteracting vascular endothelial growth factor (VEGF)-induced permeability in acute myocardial infarction [10]. It has also been reported that recombinant human ANGPTL4 (rhANGPTL4) modulates endothelial permeability and improves the endothelial network following ischemia/reperfusion brain injury, indicating a preservative effect on the vasculature and inhibition of edema during stroke [11]. VEGF-mediated vascular permeability (VP) contributes to the formation of edema in the infarct border zone within several hours following an acute ischemic event via the Src signaling pathway downstream from VEGF receptor 2 (VEGFR2) [12,13]. However, it remains unknown whether ANGPTL4 is able to reduce edema induced by ICH.

Therefore, the aim of the present study was to investigate whether rhANGPTL4 reduces hematoma volume and improves mouse neurological function in a mouse model of ICH. The researchers also explored the possible mechanisms underlying ANGPTL4 restorative effects.

Material and Methods

Experimental animals and intracerebral hemorrhage induction

The Institutional Animal Care and Use Committee of Tongji Medical College at Huazhong University of Science and Technology (Wuhan, China) approved the experiments performed in the present study. Experiments were performed in accordance with the guidelines of the Institute of Laboratory Animal Resources (Washington, DC, USA). A total of 168 12-week-old male C57BL/6J mice weighing 25–28 g were purchased from the Tongji Medical College Experimental Animal Center (Wuhan, China) for use in the present study. The animals were housed in a controlled environment at a temperature of 22–24°C and a humidity of 40–50%, with a 12-h light/dark cycle and free access to food and water. Mice were randomly assigned to receive a single intravenous injection of rhANGPTL4 (0.5 mg/ml in sterile saline) (i.v., 40 µg/kg) or an equal volume of saline in the tail vein 5 min prior to surgery. Data analysis was performed under blinded or double-blinded conditions. Mice in the current study had a mortality rate of 10.7% due to ICH injury and surgery failure. All 18 mice that died were eliminated from subsequent data analyses.

Experimental ICH was induced via intrastriatal injection of bacterial collagenase (VII-S; Sigma-Aldrich; Merck KGaA, Darmstadt, Germany) as previously described [14]. Mice were anesthetized with 10% chloral hydrate (Sigma-Aldrich; Merck KGaA, Darmstadt, Germany) (35 mg/kg) intraperitoneally and were secured in a prone position using a stereotaxic frame (RWD Life Science Co., Ltd., San Diego, USA). A scalp incision was made along the midline and a 1-mm burr hole was subsequently drilled into the right side of the skull. A 26G needle was vertically inserted into the striatum through the burr hole (1.0 mm posterior to the bregma, 2.0 mm lateral, and 3.7 mm below the dura) and bacterial collagenase (VII-S; 0.2 U dissolved in 2.0 µl phosphate buffer saline) was injected using a Microliter syringe (RWD Life Science Inc., San Diego, CA, USA) at a rate of 0.5 µl/min. The syringe needle was left in place for an additional 15 min to prevent collagenase backflow along the needle tract. The syringe was withdrawn at a rate of 1 mm/min, the burr hole was sealed with bone wax (Medline Industries, Inc., California, USA), and the scalp suture closed. All mice were allowed to fully recover under observation. The groups used in the present study were as follows: ANGPTL4 group (40 µg/kg rhANGPTL4, ICH, n=72), control group (saline, ICH, n=72), and sham group (saline, sham surgery, n=6). The sham group was only used to observe microstructures via transmission electron microscopy.

Neurofunctional assessments

Rotarod test

All behavioral testing was conducted prior to surgery and at 1, 3, 7, 14, 21, and 28 days post-surgery. The rotarod test is typically used to assess sensorimotor coordination and balance [15,16]. Mice were placed on a rod that accelerated smoothly from 0 to 30 rpm over a period of 5 min. The amount of time that each mouse was able to remain on the rod was recorded as the latency to fall. Preoperative training was performed daily for 5 consecutive days, and the results of the 3 trials prior to surgery were used as a baseline. The mean of 3 trials was used to represent each mouse's daily performance for the baseline and postsurgical evaluations.

Modified neurologic severity score (mNSS)

The mNSS test was used to assess sensory, reflex, balance, and motor deficits, as previously described [17], and was monitored by blinded investigators. Neurological function was graded on a scale of 0 to 18 (normal score=0; maximal deficit score=18), with a higher score indicating a more severe injury. For the severity scores of injury, 1 point was awarded for a specific abnormal behavior or lack of a tested reflex.

Corner turn test (CTT)

The CTT was performed as previously described [7, 18]. Mice were allowed to proceed into a 30° corner. To exit the corner, animals had to turn to either the right or left, typically by rearing along the corner wall. This was repeated 10 times, with at least 30 s between trials. The score was then calculated using the following formula: (Number of right turns/all turns) ×100. Only turns involving a full rearing along either wall were recorded.

Evaluation of brain water content and hematoma volume

Brain water content (brain edema) was determined using the wet weight/dry weight method as previously described [19]. Briefly, mice under 10% chloral hydrate (50 mg/kg) anesthesia administered intraperitoneally were decapitated at 1, 3, and 7 days post-surgery. There were 6 mice at each time-point with in both groups. Brain specimens were quickly removed and divided into 3 parts: the ipsilateral hemisphere, the contralateral hemisphere, and the cerebellum. The cerebellum was used as an internal control for brain water content. All specimens were weighed on an electronic analytical balance (Sartorius BS 210 S; Sartorius UK Ltd., Epsom, UK) prior to and following drying (at 110°C for 24 h). Brain water content (%) was calculated using the following formula: (Wet-dry brain weight)/wet brain weight.

Hematoma size was evaluated by means of hematoxylin-eosin stained cryosections that were obtained at 24 h post-surgery, as described previously [18]. Mice were deeply anesthetized with 10% chloral hydrate (i.p., 35mg/kg) and transcardially perfused with ice-cold PBS followed by a 4% formaldehyde solution. There were 6 mice at this point in each group. Brains were subsequently removed, post-fixed in fresh 4% formaldehyde solution at 4°C overnight, and immersed in 30% sucrose until they sank. Frozen coronal brain sections of 10 mm in thickness were cut on a cryostat (CM3050S; Leica Microsystems Inc., Buffalo Drive, IL, USA), mounted onto poly-lysine coated glass slides, and stained with hematoxylin and eosin.

Immunofluorescence

Frozen sections were removed from the freezer, and brain slices were fixed with 4% paraformaldehyde for 15 min, then incubated with a blocking buffer (1X PBS/5% normal goat serum/0.3% Triton X-100, Servicebio Technology Co., LTD, Wuhan, China) for 30 min at room temperature. Sections were subsequently incubated at 4°C overnight with the following primary antibodies: rabbit monoclonal anti-vascular endothelial cadherin (catalogue no. ab33168, dilution, 1: 400; Abcam, Cambridge, MA, USA) and mouse monoclonal anti-Claudin-5 (catalogue no. 35-2500, dilution, 1: 50; Invitrogen, Thermo Fisher Scientific, Inc., Waltham, MA, USA). Sections were washed 6 times ×5 min with PBS and incubated with the following secondary antibodies: Alexa Fluor 594 goat anti-rabbit IgG (H+L; catalogue no. #8889, dilution,1: 400; Cell Signaling Technology, Danvers, MA, USA), and DyLight 350 conjugated goat anti-mouse IgG (catalogue no. A23010, dilution, 1: 100, Abbkine, Inc., Redlands, CA, USA) for 1 h at room temperature. For Isolectin-B4 staining, slices were incubated with Isolectin-B4 Alexa 488 conjugate (catalogue no. I21411, dilution, 1: 400; Invitrogen; Thermo Fisher Scientific, Inc.) overnight at 4°C. Images were obtained using a fluorescence microscope (BX51; Olympus Corporation, Tokyo, Japan). Image processing was performed using Photoshop CS6 software (Adobe Systems, Inc., San Jose, CA, USA).

Transmission electron microscopy (TEM)

Mice in the sham group, the ANGPTL4 group, and the control group at 24 h and 72 h post-ICH were anesthetized with 10% chloral hydrate (i.p., 50 mg/kg) and decapitated. To avoid mechanical disruption of the blood capillaries, perfusion was not performed [20]. The tissues in the scope of 1 mm around the hematoma were separated, sliced into pieces 1 mm thick in one dimension, fixed in 2.5% glutaraldehyde in a 0.1 M cacodylic acid buffer (catalogue no. N11779; Sigma-Aldrich; Merck KGaA, Darmstadt, Germany) (pH 7.3) overnight at 4°C, and post-fixed in 2% osmic acid (catalogue no. O5500; Sigma-Aldrich; Merck KGaA, Darmstadt, Germany) for 2 h. The tissues were dehydrated using graded ethanol soaked in a mixed liquor of

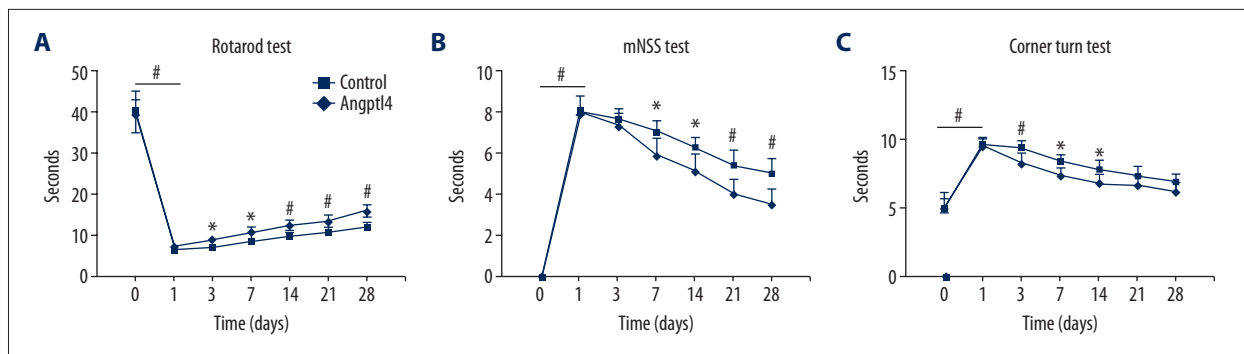


Figure 1. All animals exhibited similar and marked neurological impairments at day 1 following ICH. **(A)** Rotarod test. Rotarod score was significantly lower for mice in the control group compared with the ANGPTL4 group from day 3 following ICH. **(B)** mNSS test. Significant behavioral improvement was observed in ANGPTL4-treated mice compared with the control group from day 7 following ICH. **(C)** Corner turn test. Significant differences were observed between groups from day 3 to day 14; however, no significant difference was observed at days 1, 21, and 28. Data are presented as the mean±standard deviation, n=8 mice/group/test, * P<0.05, and # P<0.01 vs. ANGPTL4. ANGPTL4 – angiotensin-like 4; ICH – intracerebral hemorrhage; mNSS – modified neurological severity score.

epoxy resin and acetone for 24 h at 37°C. Tissues were embedded in Epon812 for 24 h, cut into semi-thin sections (5 µm), and stained with toluidine blue to determine the range of observation. Slices were then cut into ultrathin sections (60 nm), mounted on copper grids, and stained with uranyl acetate and lead nitrate for 2 h at room temperature. Sections were examined and images were captured using a Tecnai G20 TWIN transmission electron microscope (FEI; Thermo Fisher Scientific, Inc.).

Western blotting

Total proteins from the contralateral and ipsilateral striatum were separately extracted using a ProteoPrep Total Extraction Kit (catalogue no. G2001; Servicebio Technology Co., LTD, Wuhan, China) according to the manufacturer's protocol. Protein concentration of each sample was determined using the bicinchoninic acid assay (Sigma-Aldrich; EMD Millipore). Protein samples (20 µg per lane) were separated by 10% SDS-PAGE and transferred to polyvinylidene difluoride membranes, then incubated with 3% BSA (catalogue no. G5001; Servicebio Technology Co., LTD, Wuhan, China) for 2 h at room temperature. Four primary antibodies were incubated with the membranes overnight at 4°C: rabbit monoclonal anti-VE-cadherin (1: 1000), mouse monoclonal anti-Claudin-5 (1: 1000), mouse monoclonal anti-Src (catalogue no. 2115, dilution, 1: 1000; Cell Signaling Technology, Danvers, MA, USA), and rabbit monoclonal anti-phospho-Src (catalogue no. 2101, dilution, 1: 1000; Cell Signaling Technology, Danvers, MA, USA). Membranes were washed 6 times ×5 min with PBS and subsequently incubated with the following secondary antibodies: goat anti-rabbit horseradish peroxidase-conjugated IgG (catalogue no. AB501, dilution, 1: 3000; Novoprotein, Shanghai, China) and goat anti-mouse horseradish peroxidase-conjugated IgG (catalogue no. GB23301, dilution, 1: 2500; Servicebio Technology

Co., LTD, Wuhan, China). Immunoblots were visualized using enhanced chemiluminescence Plus Western Blotting Detection Reagents (Beyotime Institute of Biotechnology, Beijing, China). Antibodies against β-actin (catalogue no. 4970, dilution, 1: 1000; Cell Signaling Technology, Danvers, MA, USA) were employed as the loading control. Every group had 8 replicates performed following the steps above. Densitometry analysis was performed using Image J software (version 2x; Rawak Software, Inc., Germany), with normalization to β-actin.

Statistical analysis

Data are presented as the mean ± standard deviation. A repeated-measures analysis of variance (ANOVA) test was used for comparison of the mean scores within each group to determine the treatment effect on the behavior score at the different time-points. Student's t-test was used for comparisons between 2 groups. For multiple comparisons, a one-way ANOVA was used. Statistical analysis was performed using SPSS 21.0 (IBM SPSS, Armonk, NY, USA). Figures were created using GraphPad Prism 6.0 (GraphPad Software, Inc., La Jolla, CA, USA). P<0.05 was considered to indicate a statistically significant difference.

Results

ANGPTL4 ameliorates ICH-induced neurological deficits

The results of the rotarod, mNSS, and CTT are presented in Figure 1. There were significant differences between the ANGPTL4 group and the control group in the 3 tests (the group effect: P=0.001, P=0.008, P=0.015, respectively). All ICH mice exhibited similar and marked neurological impairments at day 1

after injury, with no significant differences between the control group and the ANGPTL4 group ($P < 0.05$, Figure 1A–1C). However, motor function and coordination in the ANGPTL4-treated group improved compared with the control group over time.

For the rotarod test, the basal mean score of the 12 subjects was 40.06 ± 3.99 s. The scores in both groups in the rotarod test decreased significantly to 6.88 ± 1.09 s at day 1 following ICH ($P < 0.05$). However, from day 3 until day 28 following treatment, the mean score improved significantly in the ANGPTL4-treated group compared with the control group and markedly improved compared with the previous time-points. The functional improvement in the control group was weaker than in the ANGPTL4-treated group throughout the follow-up period (days 7 and 14, $P < 0.05$; days 21 and 28, $P < 0.01$; Figure 1A).

For the mNSS test, the basal mean score of the 12 subjects was 0 ± 0.5 , and all mice demonstrated clear dysfunction following ICH (scores of 8.00 ± 0.73 , $P < 0.05$). However, the scores of the ANGPTL4-treated group were significantly lower than those of the control group from day 7 to day 28 post-surgery (days 7 and 14, $P < 0.05$; days 21 and 28, $P < 0.01$; Figure 1B). This improvement was progressive throughout the follow-up, with only moderate improvement observed in the control group (Figure 1B).

The ANGPTL4-treated mice had a lower CTT score at days 3, 7, and 14 relative to the control ($P = 0.004$, $P = 0.040$, $P = 0.045$ respectively; Figure 1C); however, no significant improvement was observed at days 1, 21, or 28. The results of the 3 tests indicate that ANGPTL4 has a restorative effect on neurological deficits following brain injury due to ICH.

ANGPTL4 reduces hematoma volume and brain edema associated with ICH

Histopathological staining revealed marked brain tissue damage in and around the hematoma in the ICH model following intrastriatal collagenase injection (Figure 2A). The ANGPTL4 significantly decreased the hemorrhage volume at 3 days following ICH compared with the control group ($P < 0.01$; Figure 2B).

Brain water content was measured at 1, 3, and 7 days following ICH. The water content of the ipsilateral hemisphere in the control group was significantly increased compared with the contralateral hemisphere at 1, 3, and 7 days following ICH ($P < 0.01$, Figure 2E). The peak of the ipsilateral brain edema was at 3 days following ICH in both groups ($P < 0.01$; Figure 2D); then the water content began to decrease, and at 7 days it was still higher than that on the contralateral side ($P < 0.05$; Figure 2D). However, in the ANGPTL4-treated mice, this increase was prevented at 1 and 3 days following surgery compared with the control mice ($P < 0.05$; Figure 2D), and at 7

days no difference was found compared with the contralateral side (Figure 2F). No significant difference was detected in the water content of the contralateral hemispheres and the cerebella of both groups at 3 days following ICH (Figure 2C). These results suggest that ANGPTL4 inhibits the expansion of hematoma volume and the degree of brain edema in the perihematoma area.

ANGPTL4 protects interendothelial junctions from disruption following ICH

ICH induces disruption of cell-cell junctions, vascular leakage, and edema formation in perihematomal areas. To quantify adherens and tight junction staining independently of the preservation of the vascular endothelial network, VE-cadherin and claudin-5 areas were normalized to the total endothelial cell surface area (assessed by Isolectin-B4 staining) and expressed as a percentage (Figure 3) [11]. VE-cadherin and claudin-5-positive areas were significantly larger in the perihematomal areas of ANGPTL4-treated mice than in those of control mice (both $P < 0.01$; Figure 3B, 3C). These results indicate that ANGPTL4 specifically protects against ICH-induced VE-cadherin and claudin-5 disruption following stroke.

ANGPTL4 attenuated damage to the BBB ultrastructure

In the sham group, the ultrastructure of the basal laminae was found to be continuous and integrated, and the endothelial cells and tight junctions were normal (Figure 4A). All capillaries consisted of a single layer of endothelial cells forming a lumen surrounded by a single layer of basement membrane. Several erythrocytes were observed in the lumen of the capillaries (Figure 4B). Astrocytes appeared to be in close contact with the capillaries. Organelles in all cells were all preserved, and mitochondria had a normal pattern of cristae. There was no swelling or vacuolization of the mitochondria (Figure 4A, 4B).

In the control group, the basal laminae were locally collapsed, and the endoplasmic reticulum and mitochondria were dilated at 1 day following ICH. Mitochondria with severely swollen and disorganized cristae were observed in the cytoplasm of all cells, including endothelial cells (Figure 4C). The basal laminae were more seriously collapsed; angioedema was evident and gradually became aggravated at 3 days post-surgery. Furthermore, the astrocyte foot processes appeared swollen, and the structure of the endoplasmic reticulum and mitochondria were indistinct, even collapsed (Figure 4D). For the ANGPTL4 group, slight changes were noted at 1 and 3 days following ICH compared with the control group. Mitochondria with mild swollen cristae were observed in endothelial cells at 1 and 3 days following ICH, but no collapsing of mitochondria or ER was observed (Figure 4E, 4F). These results suggest that ANGPTL4 can protect the BBB against ICH-induced destruction.

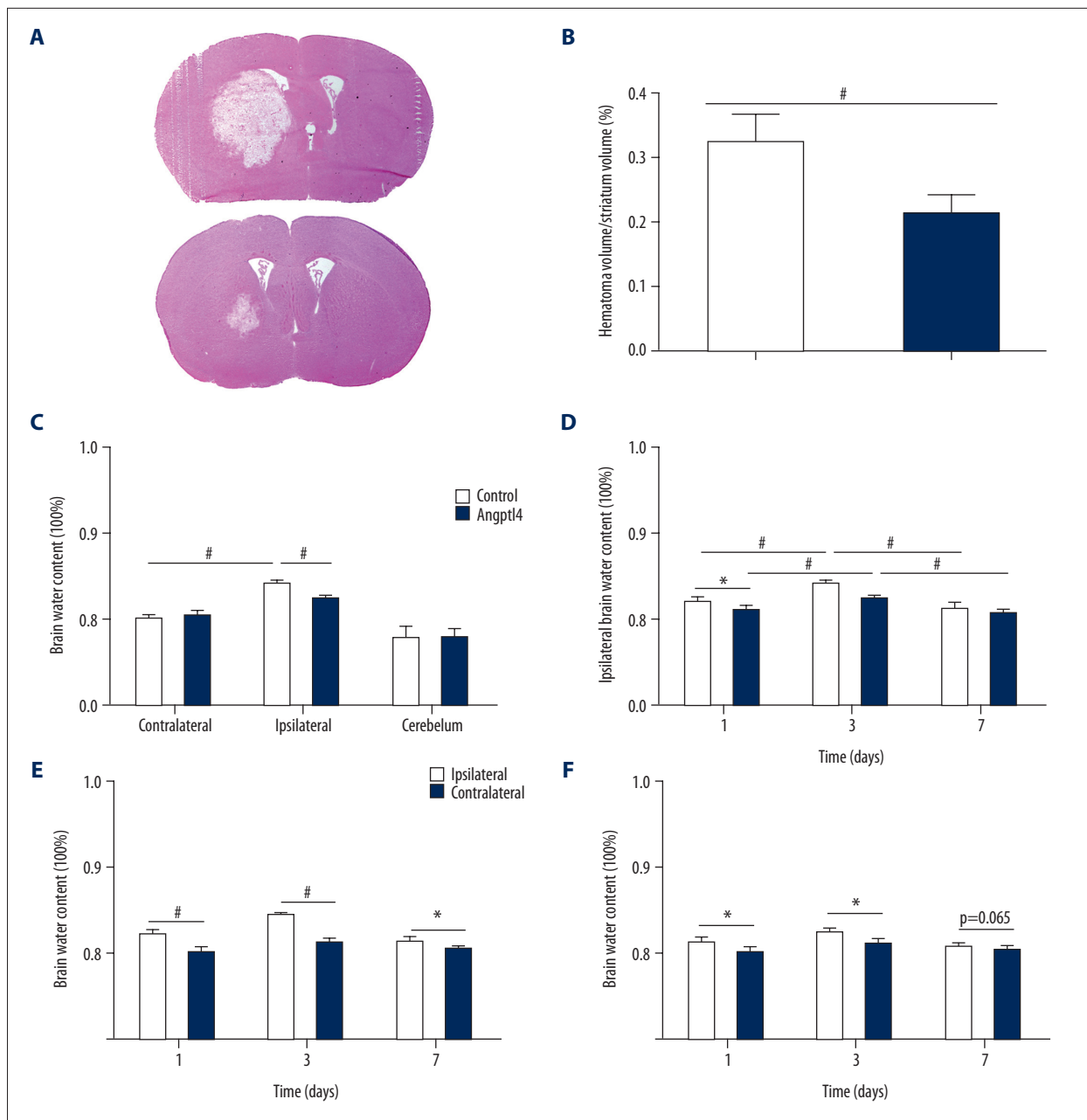


Figure 2. ANGPTL4 decreased brain damage and edema formation induced by ICH. **(A)** Hematoxylin and eosin staining revealed tissue damage in the contralateral and ipsilateral striata of control and ANGPTL4-treated mice following intrastriatal collagenase injection. No tissue damage was observed in the contralateral striata. **(B)** Quantification of hematoma volume normalized to the striatum volume in control and ANGPTL4-treated mice. **(C)** Brain water content of contralateral and ipsilateral hemispheres and the cerebellum in both groups at 3 days following ICH. **(D)** Brain water content of the ipsilateral hemispheres of control and ANGPTL4-treated mice at 1, 3, and 7 days following ICH. **(E)** The difference in brain water content between ipsilateral and contralateral hemispheres in the control group at 1, 3, and 7 days following ICH. **(F)** The difference in brain water content between ipsilateral and contralateral hemispheres in group at 1, 3, and 7 days following ICH. Data are presented as the mean \pm standard deviation. (Hematoxylin-eosin, n=6 mice/group; Brain water content, n=8 mice/group/time-point). * $P < 0.05$ and # $P < 0.01$. ANGPTL4 – angiotensin-like 4; ICH – intracerebral hemorrhage.

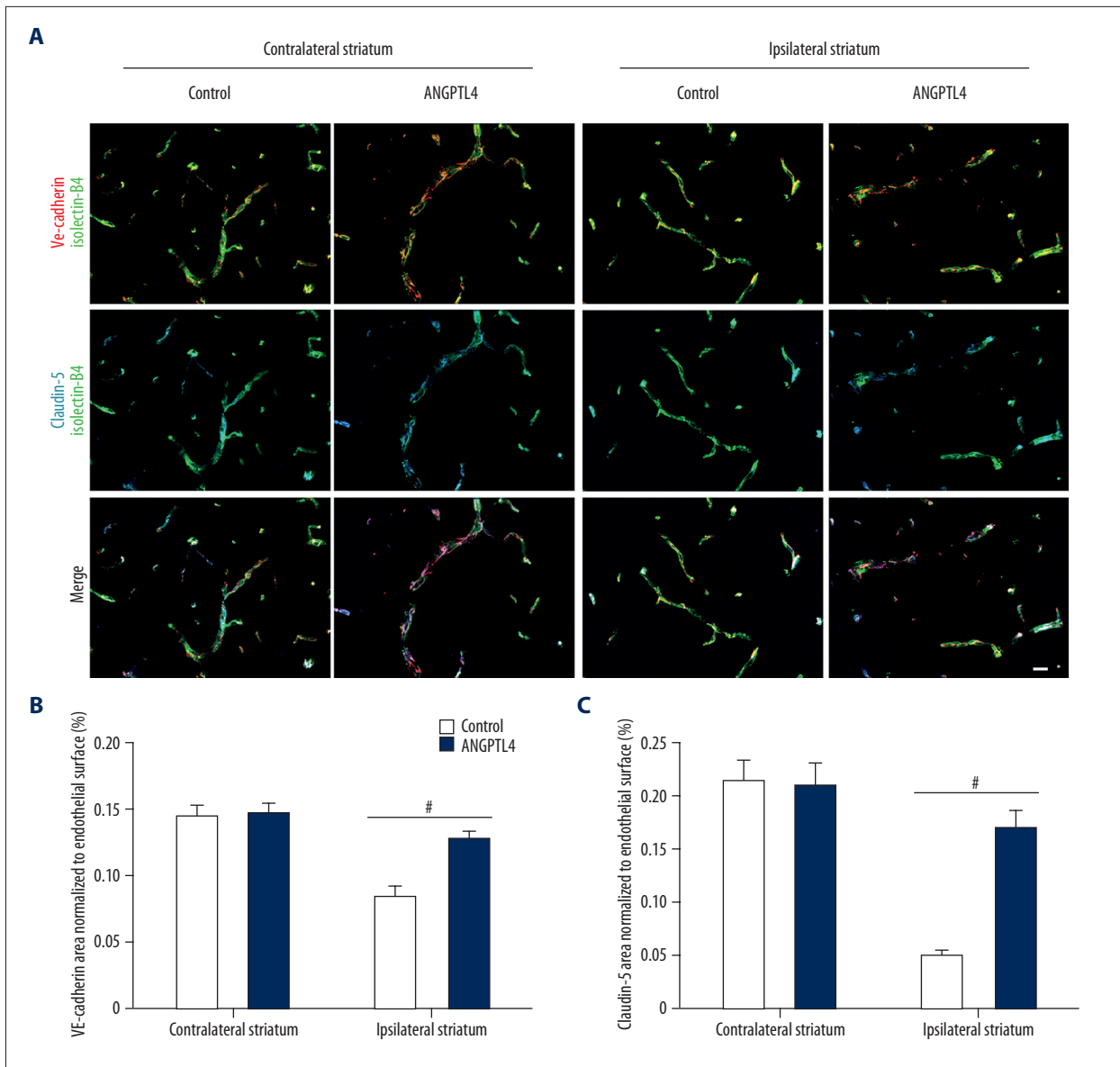


Figure 3. ANGPTL4 specifically protected interendothelial junctions in ICH. **(A)** Immunostaining of VE-cadherin and claudin-5 in contralateral and ipsilateral striata of control and ANGPTL4-treated mice. Quantification of **(B)** VE-cadherin- and **(C)** claudin-5-positive areas normalized to the total EC surface area (Isolectin B4 staining) in contralateral and ipsilateral striata of control and ANGPTL4-treated mice. Data are presented as mean ± standard deviation. Magnification: ×400, Scale bar=20 μm. n=6 mice/group, # P<0.01. ANGPTL4 – angiopoietin-like 4; ICH – intracerebral hemorrhage; VE – vascular endothelial; EC – endothelial cells.

The underlying mechanisms of ANGPTL4 ICH

Because adherens junction proteins and tight junction proteins contribute to the integrity of the BBB, the expressions of VE-cadherin and claudin-5 were assessed using Western blotting (Figure 5A). Western blot analysis confirmed that there was a significant increase in VE-cadherin (P<0.01; Figure 5B) and claudin-5 levels (P<0.01; Figure 5C) in the perihematomal areas of ANGPTL4-treated mice compared with control mice. Previous

studies have confirmed that Src kinase plays a role in dissociating the VEGFR2-VE-cadherin complex in stroke [12,21]. To determine whether ANGPTL4 influences the level of edema by inhibiting Src-mediated VP, the expressions of Src and phospho-Src were also examined using Western blot assays. The results demonstrate that ANGPTL4 significantly reduces the ratio of phospho-Src to Src (P<0.01; Figure 5D).

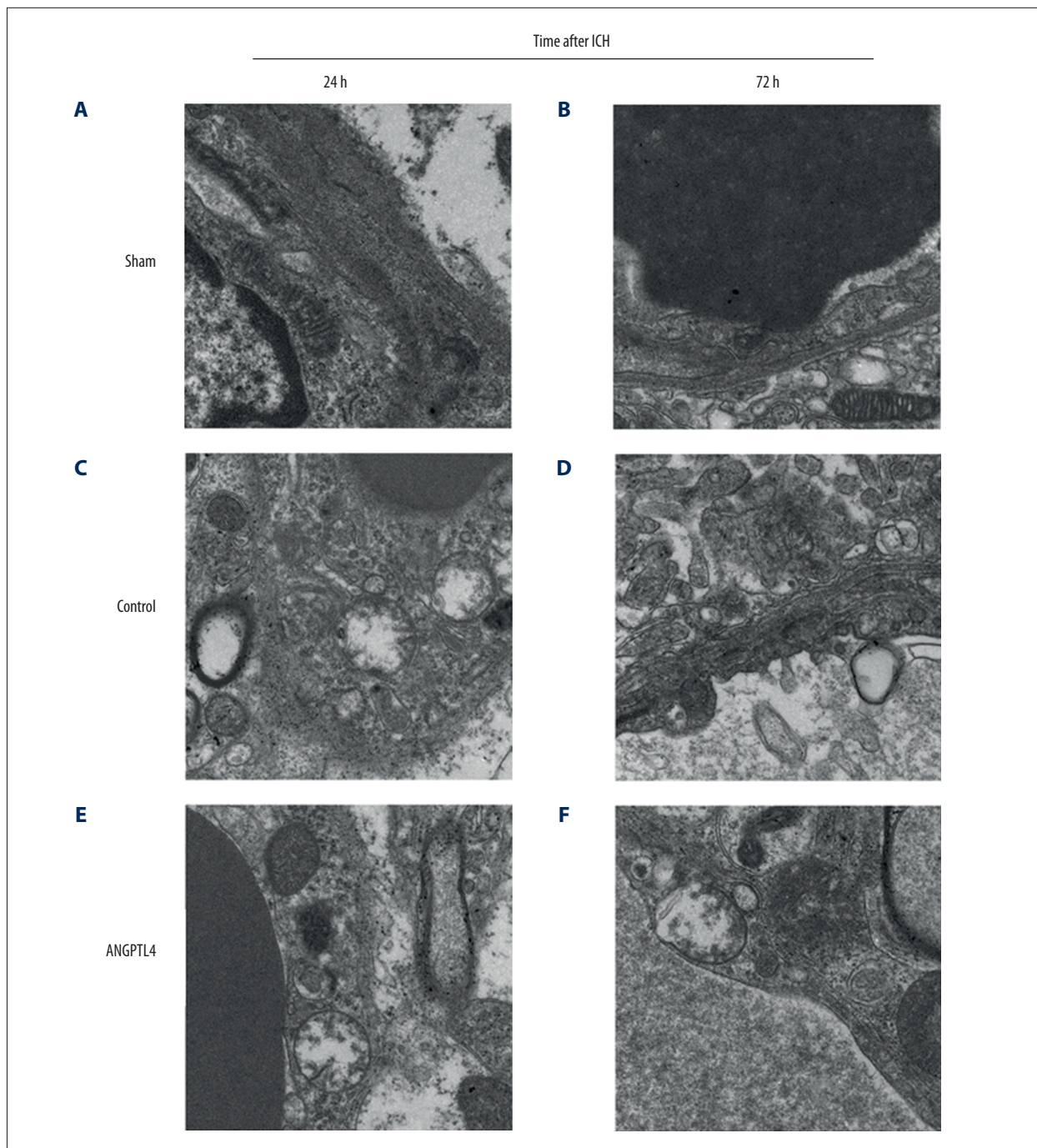


Figure 4. Electron microscopy images of the striata from C57BL/6J mice at 24 and 72 h following ICH. **(A, B)** Representative images derived from the perihematoma tissue of sham mice revealed a normal blood-brain barrier structure. **(C)** Markedly swollen astrocytic processes and mitochondria with disorganized cristae were observed in the cytoplasm of all cells around the capillaries in control mice at 1 day following ICH. **(D)** The structure of basal laminae, astrocytic foot processes, and mitochondria were indistinct, even collapsed, in control mice at day 3 following ICH. **(E, F)** Mitochondria with moderate swollen cristae were observed in endothelial cells in ANGPTL4-treated mice at days 1 and 3 following ICH. Magnification: $\times 7800$. $n=3$ mice/group/time-point. ANGPTL4 – angiotensin-like 4; ICH – intracerebral hemorrhage.

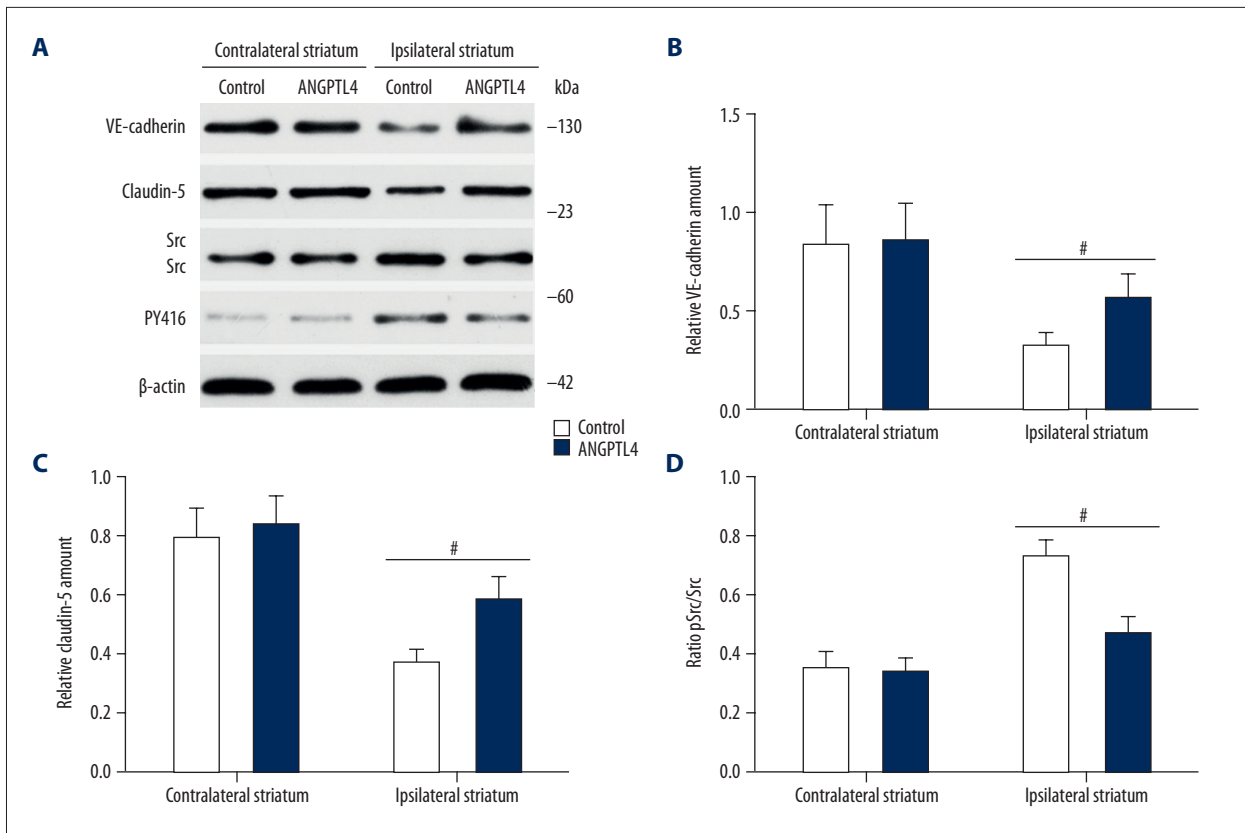


Figure 5. ANGPTL4 specifically protected against ICH-induced VE-cadherin and claudin-5 disruption following stroke. **(A)** Representative Western blot of protein expressions in the perihematoma regions 24 h following ICH. Relative density was normalized with β -actin and quantified using Image J software. A significant increase in **(B)** VE-cadherin and **(C)** claudin-5 levels was observed in the ipsilateral striata of ANGPTL4-treated mice. **(D)** ANGPTL4 significantly attenuated the level of pSrc compared with the control mice. Data are presented as the mean \pm standard deviation. $n=6$ mice/group, # $P<0.01$. ANGPTL4 – angiotensin-like 4; ICH – intracerebral hemorrhage; VE – vascular endothelial; p – phosphorylated.

Discussion

It is well known that BBB breakdown is involved in hemorrhagic stroke and hemorrhage transformation of ischemic stroke [22]. In animal models, perihematoma brain edema typically develops within hours, peaks at several days post-ICH, and subsequently decreases slowly [23]. Several studies have demonstrated that attenuation of brain edema promotes the recovery of neurological function [24,25]. Hematoma volume is also a predictive factor of poor outcome after ICH [26]. In the present study, the water content of the ipsilateral hemisphere in ANGPTL4-treated mice was lower than that of control mice at 1 and 3 days following ICH. Furthermore, the neuroscore reveals that neurofunctional deficits were significantly greater in control mice that did not receive ANGPTL4. These data demonstrate that ANGPTL4 can attenuate perihematoma brain edema and hematoma volume, as well as improve neurofunctional deficits in mice after experimentally-induced ICH.

The BBB is a physical barrier preventing the movement of molecules between the blood and the brain, and disruption of the BBB following ICH contributes to the development of brain edema [27,28]. VE-cadherin, a transmembrane protein that is anchored in the cytoskeleton, is a major component of the adherens junctions in endothelial cells (EC) and is required to maintain vascular integrity and barrier function [29]. It has been demonstrated that tight junction proteins containing claudin-5 exist in cerebral vascular endothelial cells, and they serve a critical role in maintaining BBB integrity [30]. The results of the present study provide evidence that ANGPTL4 protects interendothelial junctions from disruption, as demonstrated by immunofluorescence and Western blot analyses. These data indicate that ANGPTL4 protects against vascular structure damage and specifically protects against ICH-induced VE-cadherin and claudin-5 disruption following stroke.

Perihematoma perfusion is reduced in the ipsilateral hemisphere of all patients with acute ICH compared with contralateral hemisphere regional cerebral blood flow (rCBF) [31,32].

Hypoxic conditions result in the stimulation of hypoxia-inducible factors, which translocate to the nucleus to bind hypoxia response elements in target genes and promote the production of VEGF [33]. One study demonstrated that activated platelets often deposit high levels of VEGF [34]. Another study proposed that VEGF released from activated platelets at the site of hemorrhage may interact with thrombin to increase vascular permeability and contribute to the development of edema [22]. It has also been reported that ischemic-induced VEGF binds to VEGFR2 and dissociates the VEGFR2-VE-cadherin complex via the Src signaling pathway, leading to interendothelial junction disruption and promoting vascular leakage [12]. Blocking Src activity within the first 6 h following ischemic stroke reduces edema and improves outcomes [35]. A previous study reported that mice deficient in pp60Src exhibited no vascular permeability response to VEGF, and they exhibited minimal edema and infarction volume following stroke [21]; however, there was no influence on the angiogenic response to VEGF [36]. VEGF is associated with VP, and, consequently, brain edema formation following cerebral ischemia and ICH. In the present study, changes in the Src signaling pathway downstream from VEGFR2 were evaluated. The results demonstrated that ANGPTL4 inhibited disruption of the BBB by interrupting Src phosphorylation, retaining the adherens junction proteins at the cell-cell junctions, and preserving endothelial barrier function.

Further studies are required to confirm the relevance of targeting interendothelial EC junctions to reduce permeability using ANGPTL4 treatment. A recent study has found that no awakening after sICH (supratentorial intracerebral hemorrhage, sICH)

with coma is potentially caused by sepsis-associated encephalopathy (SAE) [37], and research is needed to determine if ANGPTL4 can inhibit inflammatory response and promote the restoration of damaged neurons, and, if so, the possible mechanisms of such a restoration.

Conclusions

The present study is the first to investigate the potential of ANGPTL4 for the treatment of ICH. Inhibiting vascular leaks by blocking Src activity may have a profound effect on reducing tissue injury. These results have revealed a molecular mechanism accounting for the Src requirement in ICH-mediated permeability and provide a basis for Src inhibition as a therapeutic option for patients at the acute phase of ICH. This may be useful for preventing hemorrhage exacerbation following ICH.

Acknowledgements

The authors would like to thank Professor Chunxiang Yang (Beijing Hualian Group, Beijing, China) for his comments on the manuscript and associate Professor Rifeng Jiang (Union Hospital, Fujian Medical University, Fuzhou, China) for his technical assistance.

Conflict of interest

None.

References:

1. Adeoye O, Broderick JP: Advances in the management of intracerebral hemorrhage. *Nat Rev Neurol*, 2010; 6: 593–601
2. van Asch CJ, Luitse MJ, Rinkel GJ et al: Incidence, case fatality, and functional outcome of intracerebral haemorrhage over time, according to age, sex, and ethnic origin: A systematic review and meta-analysis. *Lancet Neurol*, 2010; 9: 167–76
3. Qureshi AI, Tuhim S, Broderick JP et al: Spontaneous intracerebral hemorrhage. *N Engl J Med*, 2001; 344: 1450–60
4. Liao KH, Sung CW, Huang YN et al: Therapeutic potential of drugs targeting pathophysiology of intracerebral hemorrhage: From animal models to clinical applications. *Curr Pharm Des*, 2017; 23: 2212–25
5. Xi G, Strahle J, Hua Y et al: Progress in translational research on intracerebral hemorrhage: is there an end in sight? *Prog Neurobiol*, 2014; 115: 45–63
6. Lim-Hing K, Rincon F: Secondary hematoma expansion and perihemorrhagic edema after intracerebral hemorrhage: From bench work to practical aspects. *Front Neurol*, 2017; 8: 74
7. Hua Y, Schallert T, Keep RF et al: Behavioral tests after intracerebral hemorrhage in the rat. *Stroke*, 2002; 33: 2478–84
8. Eltzschig HK, Eckle T: Ischemia and reperfusion – from mechanism to translation. *Nat Med*, 2011; 17: 1391–401
9. Zhu P, Goh YY, Chin HF et al: Angiotensin-like 4: A decade of research. *Biosci Rep*, 2012; 32: 211–19
10. Galaup A, Gomez E, Souktani R et al: Protection against myocardial infarction and no-reflow through preservation of vascular integrity by angiotensin-like 4. *Circulation*, 2012; 125: 140–49
11. Bouleti C, Mathivet T, Coqueran B et al: Protective effects of angiotensin-like 4 on cerebrovascular and functional damages in ischaemic stroke. *Eur Heart J*, 2013; 34: 3657–68
12. Weis S, Shintani S, Weber A et al: Src blockade stabilizes a Flk/cadherin complex, reducing edema and tissue injury following myocardial infarction. *J Clin Invest*, 2004; 113: 885–94
13. Weis SM, Cheresh DA: Pathophysiological consequences of VEGF-induced vascular permeability. *Nature*, 2005; 437: 497–504
14. Ma Q, Manaenko A, Khatibi NH et al: Vascular adhesion protein-1 inhibition provides antiinflammatory protection after an intracerebral hemorrhagic stroke in mice. *J Cereb Blood Flow Metab*, 2011; 31: 881–93
15. Lee HJ, Park IH, Kim HJ et al: Human neural stem cells overexpressing glial cell line-derived neurotrophic factor in experimental cerebral hemorrhage. *Gene Ther*, 2009; 16: 1066–76
16. Jeong SW, Chu K, Jung KH et al: Human neural stem cell transplantation promotes functional recovery in rats with experimental intracerebral hemorrhage. *Stroke*, 2003; 34: 2258–63
17. Otero L, Zurita M, Bonilla C et al: Late transplantation of allogeneic bone marrow stromal cells improves neurologic deficits subsequent to intracerebral hemorrhage. *Cytotherapy*, 2011; 13: 562–71
18. Krafft PR, McBride DW, Lelic T et al: Correlation between subacute sensorimotor deficits and brain edema in two mouse models of intracerebral hemorrhage. *Behav Brain Res*, 2014; 264: 151–60
19. Wei S, Sun J, Li J et al: Acute and delayed protective effects of pharmacologically induced hypothermia in an intracerebral hemorrhage stroke model of mice. *Neuroscience*, 2013; 252: 489–500

20. Garbuzova-Davis S, Haller E, Saporta S et al: Ultrastructure of blood-brain barrier and blood-spinal cord barrier in SOD1 mice modeling ALS. *Brain Res*, 2007; 1157: 126–37
21. Paul R, Zhang ZG, Eliceiri BP et al: Src deficiency or blockade of Src activity in mice provides cerebral protection following stroke. *Nat Med*, 2001; 7: 222–27
22. Sansing LH, Kaznatcheeva EA, Perkins CJ et al: Edema after intracerebral hemorrhage: Correlations with coagulation parameters and treatment. *J Neurosurg*, 2003; 98: 985–92
23. Xi G, Keep RF, Hoff JT: Pathophysiology of brain edema formation. *Neurosurg Clin N Am*, 2002; 13: 371–83
24. Nakamura T, Keep RF, Hua Y et al: Deferoxamine-induced attenuation of brain edema and neurological deficits in a rat model of intracerebral hemorrhage. *J Neurosurg*, 2004; 100: 672–78
25. Nakamura T, Kuroda Y, Yamashita S et al: Edaravone attenuates brain edema and neurologic deficits in a rat model of acute intracerebral hemorrhage. *Stroke*, 2008; 39: 463–69
26. Li Q, Liu QJ, Yang WS et al: Island sign: An imaging predictor for early hematoma expansion and poor outcome in patients with intracerebral hemorrhage. *Stroke*, 2017; 48: 3019–25
27. Keep RF, Hua Y, Xi G: Intracerebral haemorrhage: Mechanisms of injury and therapeutic targets. *Lancet Neurol*, 2012; 11: 720–31
28. Liu DZ, Sharp FR: Excitatory and mitogenic signaling in cell death, blood-brain barrier breakdown, and BBB repair after intracerebral hemorrhage. *Transl Stroke Res*, 2012; 3: 62–69
29. Dejana E, Giampietro C: Vascular endothelial cadherin and vascular stability. *Curr Opin Hematol*, 2012; 19: 218–23
30. Strazielle N, Ghersi-Egea JF: Physiology of blood-brain interfaces in relation to brain disposition of small compounds and macromolecules. *Mol Pharm*, 2013; 10: 1473–91
31. Rosand J, Eskey C, Chang Y et al: Dynamic single-section CT demonstrates reduced cerebral blood flow in acute intracerebral hemorrhage. *Cerebrovasc Dis*, 2002; 14: 214–20
32. Zazulia AR, Diringner MN, Videen TO et al: Hypoperfusion without ischemia surrounding acute intracerebral hemorrhage. *J Cereb Blood Flow Metab*, 2001; 21: 804–10
33. Schoch HJ, Fischer S, Marti HH: Hypoxia-induced vascular endothelial growth factor expression causes vascular leakage in the brain. *Brain*, 2002; 125: 2549–57
34. Salgado R, Benoy I, Bogers J et al: Platelets and vascular endothelial growth factor (VEGF): A morphological and functional study. *Angiogenesis*, 2001; 4: 37–43
35. van Bruggen N, Thibodeaux H, Palmer JT et al: VEGF antagonism reduces edema formation and tissue damage after ischemia/reperfusion injury in the mouse brain. *J Clin Invest*, 1999; 104: 1613–20
36. Eliceiri BP, Paul R, Schwartzberg PL et al: Selective requirement for Src kinases during VEGF-induced angiogenesis and vascular permeability. *Mol Cell*, 1999; 4: 915–24
37. Tong DM, Zhou YT: No awakening in supratentorial intracerebral hemorrhage is potentially caused by sepsis-associated encephalopathy. *Med Sci Monit*, 2017; 23: 4408–14